Geometrically nonlinear dynamic model for a hexagonal lattice

A. V. Porubov,[1,2] A. M. Krivtsov,[1,2] I. D. Antonov,[1,2] W. H. Müller,[3] and A. A. Sokolov[3]
[1]*Institute for Problems in Mechanical Engineering, Bolshoy 61, V. O., Saint-Petersburg, Russia*
[2]*Peter the Great St. Petersburg Polytechnic University (SPbPU), Polytechnicheskaya St., 29, Saint Petersburg, Russia*
[3]*Continuum Mechanics and Materials Theory, Technische Universität Berlin, Einsteinufer 5, 10587 Berlin, Germany*

(Received 25 April 2020; accepted 29 July 2020; published 17 August 2020)

It is shown that angular stiffness in the hexagonal lattice model plays a significant role in the geometrical nonlinear terms in the equations of the continuum limit. A geometrically nonlinear discrete model is formulated for the hexagonal lattice by considering the interaction of two sublattices. An asymptotic procedure is developed in order to obtain the nonlinear coupled equations of motion in the continuum limit of the discrete model. An interaction of longitudinal and shear plane strain waves is studied by using the solutions of the obtained equations.

DOI: 10.1103/PhysRevE.102.022209

I. INTRODUCTION

The derivation of the model equations for the strain dynamics can be based on a continuum limit of the discrete lattice model equations. This is especially efficient for materials with complicated crystalline structure [1–6]. Another application is connected with non-Fourier laws of heat conduction [7]: A hyperbolic equation, referred to as the ballistic heat equation, was obtained as a mathematical consequence of the equations of lattice dynamics [8,9]. The references on the early works related to the ballistic heat equation can be found in Ref. [8].

It is known that nonlinear discrete equations usually cannot be solved analytically. This is why pure numerical approaches are applied; see, e.g., Ref. [10]. An alternative way is to apply a combined discrete-continuum approach when a continuum limit of the discrete equations is analyzed. The obtained continuum equations of motion should correspond to those obtained when using the pure continuum approach. This is especially important for the nonlinear terms in the equations. There are at least two types of nonlinearity in the continuum equations for nonlinear strain dynamics. The first one is caused by the nonlinear dependence between the strains and the displacement derivatives, which is described by the Cauchy-Green strain tensor in the reference configuration. It is called the geometrical nonlinearity. The second type of nonlinearity accounts for deviations from Hooke's law. It is referred to as the physical nonlinearity [11].

Nonlinear modeling in lattices is mainly based on the consideration of nonlinear stiffness of the springs between the masses [10,12–18]. This corresponds to the physical nonlinearity. However, the simplest one-dimensional (1D) lattice model with masses connected by linear elastic springs, undergoing only translational displacements, does not produce continuum limit equations with the geometrically nonlinear terms [4–6]. The addition of two-dimensional (2D) motion in the 1D model, such as dipole motion [19], rotational degree of freedom [20], and effective stiffness modulation [21], may help to include a geometrical nonlinearity in the discrete model and in its continuum limit.

The hexagonal lattice has attracted considerable attention due to its applicability for a graphene modeling and possible development of new heat conduction laws. The simplest linear model takes only the translational motion of the lattice masses into account [22–24]. Angular interactions have been used in Refs. [15,25], and nonlinear modeling has been developed in Refs. [14,25]. It should be pointed out that the Cauchy-Born rule linking the continuum model with particle interaction [26] requires the atomic structure of the materials to be centrosymmetric, because such a structure ensures the equilibrium of particles in a lattice. The hexagonal arrangement of atoms does not meet this requirement: when a lattice is under "homogeneous deformation" on the cell level, the deformation may not be homogeneous inside the cell. An attempt to modify the Cauchy-Born rule to work for a hexagonal atomic structure is to introduce a rigid body translation as an internal degree of freedom. The hexagonal lattice can be decomposed into two sublattices, each of which is centrosymmetric [27].

The aim of this paper is to study nonlinear strain dynamics of the equations obtained as a continuum limit of the discrete 2D geometrically nonlinear hexagonal lattice model. The paper is organized as follows. In Sec. II the lattice is decomposed into two sublattices, and both translational and angular interactions are taken into account. This allows us to write the expressions for the energies for each sublattice and to obtain the governing discrete equations of motion by using a variational principle in Sec. III. The continuum limit results in coupled governing nonlinear continuum equations for longitudinal and shear strains. In Sec. IV the role of the angular stiffness in the nonlinear term coefficients of these equations as well as in the behavior of their localized strain wave solutions are discussed. Section V concludes and summarizes the paper.

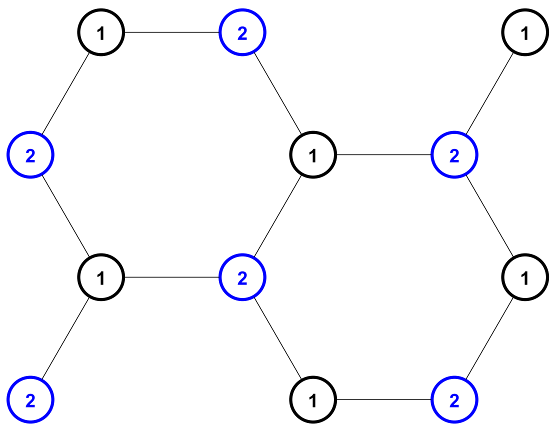

FIG. 1. Two-dimensional hexagonal lattice decomposed into two sublattices.

II. STATEMENT OF THE PROBLEM

A 2D hexagonal lattice with neighboring interactions between the masses is shown in Fig. 1. The strain processes in the lattice are based on a decomposition of the lattice into two sublattices whose elements are marked by 1 and 2. The sublattices are shown in in Figs. 2 and 3. The reason for the decompositions is related to to satisfying the Cauchy-Born rule [26,27] for the equilibrium of particles in a lattice. This rule relates the movement of atoms in a crystal to the overall deformation of the bulk solid. One needs to introduce sublattices as a way of correlating changes in positions of the entities in the lattice with descriptions of deformation used in the continuum theories of elastic phenomena. More detailed information can be found, e.g., in Refs. [26,27].

The interactions are modeled by the elastic springs. Two types of interaction are considered: translation interactions with the stiffness coefficient C_1, and the angular ones with the stiffness coefficient C_2.

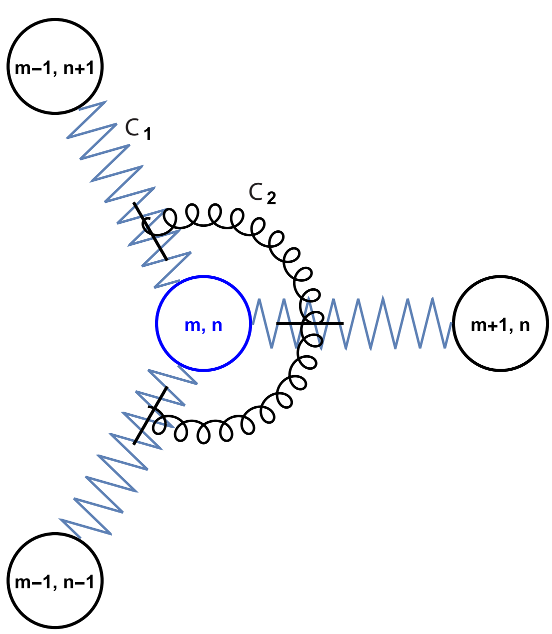

FIG. 2. First sublattice.

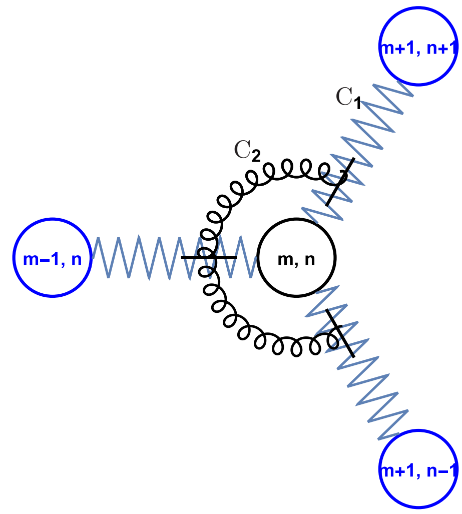

FIG. 3. Second sublattice.

The first sublattice marked by 1 in Fig. 1 with both translational and angular interactions is shown in Fig. 2. The translation displacements of a central mass corresponding to the horizontal and vertical directions are denoted by $x_{m,n}$ and $y_{m,n}$, respectively. The analogous displacements for the second sublattice are denoted by $X_{m,n}$ and $Y_{m,n}$.

The equations of motion are obtained using the Hamilton-Ostrogradsky variational principle [11]. This procedure requires knowledge of the potential strain energy, which should be defined. Both the translational and angular variations are considered while the dihedral variations [25] are omitted since no bending is considered. It is assumed that the potential energy of the interaction between the masses depends on the translational elongations and angular variations. The physical nonlinearity is omitted in our consideration since the aim is to clarify the role of the geometrical nonlinearity. It allows us to use the power series quadratic dependence on elongations. Then one obtains for the first sublattice (Fig. 2) that the energy of translational displacements is

$$\Pi_{t,1} = \frac{C_1}{2}\left(\Delta l_1^2 + \Delta l_2^2 + \Delta l_3^2\right),$$

where the translational elongations for the first sublattice, Δl_i, are

$$\Delta l_1 = \sqrt{(l + X_{m+1,n} - x_{m,n})^2 + (Y_{m+1} - y_{m,n})^2} - l,$$

$$\Delta l_2 = \left\{\left[l\,\cos\left(\frac{\pi}{3}\right) - (X_{m-1,n+1} - x_{m,n})\right]^2 + \left[l\,\sin\left(\frac{\pi}{3}\right) + (Y_{m-1,n+1} - y_{m,n})\right]^2\right\}^{1/2} - l, \quad (1)$$

$$\Delta l_3 = \left\{\left[l\,\cos\left(\frac{\pi}{3}\right) - (X_{m-1,n-1} - x_{m,n})\right]^2 + \left[l\,\sin\left(\frac{\pi}{3}\right) - (Y_{m-1,n-1} - y_{m,n})\right]^2\right\}^{1/2} - l, \quad (2)$$

where l is an equilibrium distance between the masses in the lattice.

Similarly, the energy of translational displacements in the second sublattice (Fig. 3) is

$$\Pi_{t,2} = \frac{C_1}{2}\left(\Delta L_1^2 + \Delta L_2^2 + \Delta L_3^2\right),$$

where the elongations of the second sublattice are

$$\Delta L_1 = \sqrt{(l + X_{m,n} - x_{m-1,n})^2 + (y_{m-1,n} - Y_{m,n})^2} - l,$$

$$\Delta L_2 = \left\{\left[l\,\cos\left(\frac{\pi}{3}\right) + (x_{m+1,n+1} - X_{m,n})\right]^2 + \left[l\,\sin\left(\frac{\pi}{3}\right) + (y_{m+1,n+1} - Y_{m,n})\right]^2\right\}^{1/2} - l, \quad (3)$$

$$\Delta L_3 = \left\{\left[l\,\cos\left(\frac{\pi}{3}\right) + (x_{m+1,n-1} - X_{m,n})\right]^2 + \left[l\,\sin\left(\frac{\pi}{3}\right) - (y_{m+1,n-1} - Y_{m,n})\right]^2\right\}^{1/2} - l. \quad (4)$$

The angular variation energy is considered depending on the cosines of the angles between directions from the central mass to neighbors in each sublattice [25]. Let us consider the section between masses with the indices (m, n), $(m+1, n)$ and $(m-1, n+1)$ (Fig. 2). We introduce the vectors $\mathbf{r_0}$, $\mathbf{r_{m+1}}$, $\mathbf{r_{n+1}}$, as follows:

$$\mathbf{r_0} = \mathbf{i}(l + X_{m+1,n} - x_{m,n}),$$

$$\mathbf{r_{m+1}} = \mathbf{i}(l + X_{m+1,n} - x_{m,n}) + \mathbf{j}(Y_{m+1,n} - y_{m,n}), \quad (5)$$

$$\mathbf{r_{n+1}} = -\mathbf{i}[l\cos(\pi/3) - X_{m-1,n+1} + x_{m,n}] + \mathbf{j}[l\sin(\pi/3) + Y_{m-1,n+1} - y_{m,n}], \quad (6)$$

where $\mathbf{i}$, $\mathbf{j}$ are the unit vectors in the horizontal and vertical directions, respectively. Then the angular variation of the mass $(m+1, n)$ relative to the equilibrium horizontal position, φ_1, can be characterized by the difference between the cosines corresponding to the current and equilibrium positions. For this purpose, the Law of Cosines

$$\cos(\varphi_1) - \cos(0) = \frac{\mathbf{r_{m+1}} \cdot \mathbf{r_0}}{|\mathbf{r_{m+1}}||\mathbf{r_0}|} - 1$$

is used. Similarly the angular variation, φ_2, of the mass $(m-1, n+1)$ relative to the equilibrium position $2\pi/3$ can be characterized by the difference between the cosines

$$\cos(\varphi_2) - \cos(2\pi/3) = \frac{\mathbf{r_{n+1}} \cdot \mathbf{r_0}}{|\mathbf{r_{n+1}}||\mathbf{r_0}|} + 1/2.$$

The contribution to the angular strain energy is

$$\Pi_{an,1} = C_2 l^2\{[\cos(\varphi_2) - \cos(2\pi/3)] - [\cos(\varphi_1) - \cos(0)]\},$$

where C_2 is the angular stiffness. For the section between the masses with the indices (m, n), $(m+1, n-1)$, and $(m-1, n+1)$ (Fig. 2), we also introduce the vector

$$\mathbf{r_{n-1}} = -\mathbf{i}[l\cos(\pi/3) - X_{m-1,n-1} + x_{m,n}] - \mathbf{j}[l\sin(\pi/3) - Y_{m-1,n-1} + y_{m,n}].$$

Then the angular variation, ψ, of the mass $(m-1, n+1)$ relative to the equilibrium position $-2\pi/3$ can be characterized by the difference between cosines

$$\cos(\psi) - \cos(2\pi/3) = \frac{\mathbf{r_{n-1}} \cdot \mathbf{r_0}}{|\mathbf{r_{n-1}}||\mathbf{r_0}|} + 1/2.$$

The contribution to the angular strain energy is

$$\Pi_{an,2} = C_2 l^2\{[\cos(\psi) - \cos(2\pi/3)] - [\cos(\varphi_1) - \cos(0)]\}.$$

Similarly we obtain for the second sublattice shown in Fig. 3 by introducing angular variations Φ_1, Φ_2, Ψ for the masses $(m-1, n)$, $(m+1, n+1)$, and $(m+1, n-1)$ relative to the equilibrium position, respectively,

$$\Pi_{an,3} = C_2 l^2\{[\cos(\Phi_2) + \cos(2\pi/3)] - [\cos(\Phi_1) - \cos(0)]\},$$

$$\Pi_{an,4} = C_2 l^2\{[\cos(\Psi) + \cos(2\pi/3)] - [\cos(\Phi_1) - \cos(0)]\},$$

where

$$\cos(\Phi_1) - \cos(0) = \frac{\mathbf{R_{m-1}} \cdot \mathbf{R_0}}{|\mathbf{R_{m-1}}||\mathbf{R_0}|} - 1,$$

$$\cos(\Phi_2) + \cos(2\pi/3) = \frac{\mathbf{R_{n+1}} \cdot \mathbf{R_0}}{|\mathbf{R_{n+1}}||\mathbf{R_0}|} - 1/2, \quad (7)$$

$$\cos(\Psi) + \cos(2\pi/3) = \frac{\mathbf{R_{n-1}} \cdot \mathbf{R_0}}{|\mathbf{R_{n-1}}||\mathbf{R_0}|} - 1/2, \quad (8)$$

where the corresponding expressions for angular variations in the second sublattice are

$$\mathbf{R_0} = \mathbf{i}(l + X_{m,n} - x_{m-1,n}),$$

$$\mathbf{R_{m-1}} = \mathbf{i}(l + X_{m,n} - x_{m-1,n}) + \mathbf{j}(y_{m-1,n} - Y_{m,n}),$$

$$\mathbf{R_{n+1}} = \mathbf{i}[l\cos(\pi/3) + x_{m+1,n+1} - X_{m,n}] + \mathbf{j}[l\sin(\pi/3) + y_{m+1,n+1} - Y_{m,n}],$$

$$\mathbf{R_{n-1}} = \mathbf{i}[l\cos(\pi/3) + x_{m+1,n-1} - X_{m,n}] - \mathbf{j}[l\sin(\pi/3) - y_{m+1,n-1} + Y_{m,n}].$$

The potential strain energy of the first sublattice is

$$\Pi_1 = \Pi_{t,1} + \Pi_{an,1} + \Pi_{an,2}, \quad (9)$$

the potential strain energy of the second sublattice is

$$\Pi_2 = \Pi_{t,2} + \Pi_{an,3} + \Pi_{an,4}, \quad (10)$$

the kinetic energy of the first sublattice is

$$K_1 = \frac{M}{2}\left(\dot{x}_{m,n}^2 + \dot{y}_{m,n}^2\right) + M\,l^2(\dot{\varphi}_1^2 + \dot{\varphi}_2^2 + \dot{\psi}^2), \quad (11)$$

and the kinetic energy of the second sublattice is

$$K_2 = \frac{M}{2}\left(\dot{X}_{m,n}^2 + \dot{Y}_{m,n}^2\right) + M\,l^2(\dot{\Phi}_1^2 + \dot{\Phi}_2^2 + \dot{\Psi}^2), \quad (12)$$

where M is the mass of each particle in the lattice.

III. GOVERNING EQUATIONS

A. Discrete coupled equations of motion

Making use of the Hamilton-Ostrogradsky variational principle [11] results in the coupled discrete equations for horizontal and vertical displacements. The Lagrangians are written for each sublattice as a difference between K_1 and Π_1 and K_2 and Π_2. Variation of each Lagrangian results in four equations of motion for the horizontal and vertical displacements for each sublattice.

However, the full set of equations is complicated due to nonlinear terms. The aim of this study is to obtain the continuum equations for a weakly nonlinear problem for long waves. It results in truncated power series approximations for nonlinear term expansions in the expressions for the potential and the kinetic energy. In particular, only linearized expressions for ϕ_1, ϕ_2, ψ, Φ_1, Φ_2, Ψ are used in the expressions for the kinetic energy. Omitted terms give rise to the negligibly small nonlinear terms in the continuum equations of motion. The reason for this rise will be shown in the next subsection.

The approximate discrete equations are

$$M\ddot{x}_{tt} = L_1(x, X, y, Y) + D_1(x, X, y, Y) + N_1(x, X, y, Y), \tag{13}$$

$$M\ddot{y}_{tt} = L_2(x, X, y, Y) + D_2(x, X, y, Y) + N_2(x, X, y, Y), \tag{14}$$

$$M\ddot{X}_{tt} = L_3(x, X, y, Y) + D_3(x, X, y, Y) + N_3(x, X, y, Y), \tag{15}$$

$$M\ddot{Y}_{tt} = L_4(x, X, y, Y) + D_4(x, X, y, Y) + N_4(x, X, y, Y), \tag{16}$$

where the linear discrete parts, $L_j(x, X, y, Y)$, the linear differential-discrete parts, $D_j(x, X, y, Y)$, and the nonlinear discrete parts, $N_j(x, X, y, Y)$, $j = 1$–4, are given in the Appendix. The nonlinear discrete equations are still complicated even in this weakly nonlinear case. Then the long wavelength continuum limit of them will be applied to get coupled nonlinear partial differential equations of motion.

B. Continuum limit equations

For small wave numbers (long wave approximation) one assumes that the continuum displacements of the central particle $x_{m,n}$, $y_{m,n}$ are $u(x, y, t)$, $v(x, y, t)$,

$$x_{m\pm1,n\pm1} = u \pm l\, u_x \pm l\, u_y + \frac{1}{2}l^2 u_{xx} + l^2 u_{xy} + \frac{1}{2}l^2 u_{yy} + \cdots, \tag{17}$$

etc. Similar relationships hold for the remaining variables $y_{i,k}$, $X_{i,k}$, and $Y_{i,k}$.

The 2D equations are too complicated for an analysis. The plane-wave assumption has been chosen as a first step to get model equations whose solutions might be a basis to study more complicated cases. The aim is to get model equations whose solutions might be a basis for a future study of the other kind of motions in more complicated cases.

The plan-wave assumption means that all displacements do not depend on the vertical index n,

$$x_{m\pm i,n\pm j} = x_{m\pm i}, y_{m\pm i,n\pm j} = y_{m\pm i}, X_{m\pm i,n\pm j} = X_{m\pm i},$$

$$Y_{m\pm i,n\pm j} = Y_{m\pm i}.$$

All terms with derivatives of y are absent in all approximations (17). Only the leading-order dispersion and nonlinear terms are left. Then one obtains from Eqs. (13)–(16):

$$\begin{aligned} &Mu_{tt} + \frac{3}{4}(2C_1 + 3C_2)(u - U) - \frac{l}{4}(2C_1 - 9C_2)U_x - \frac{3l^2}{8}(2C_1 + 3C_2)U_{xx} + \frac{3M}{2}(u_{tt} - U_{tt}) \\ &- \frac{l^3}{24}(2C_1 - 9C_2)U_{xxx} + \frac{3Ml}{2}U_{xtt} - \frac{l^4}{32}(2C_1 + 3C_2)U_{xxxx} - \frac{3Ml^2}{4}U_{xxtt} \\ &- \frac{81}{16l}C_2[(u - U)^2 + 2l(u - U)U_x] - \frac{3}{16l}(6C_1 - 7C_2)(v - V)^2 - \frac{1}{8}(2C_1 - 21C_2)(v - V)V_x = 0, \end{aligned} \tag{18}$$

$$\begin{aligned} &Mv_{tt} + \frac{3}{4}(2C_1 + C_2)(v - V) + \frac{3l}{4}(2C_1 + C_2)V_x - \frac{3l^2}{8}(2C_1 + C_2)V_{xx} + \frac{3M}{2}(v_{tt} - V_{tt}) \\ &+ \frac{l^3}{8}(2C_1 + C_2)V_{xxx} - \frac{Ml}{2}V_{xtt} - \frac{l^4}{32}(2C_1 + C_2)V_{xxxx} - \frac{3Ml^2}{4}V_{xxtt} - \frac{3\sqrt{3}}{2l}C_2[(v - V)^2 + 2l(v - V)V_x] \\ &- \frac{3}{8l}(6C_1 - 7C_2)(u - U)(v - V) - \frac{1}{8}(6C_1 - 21C_2)[(u - U)V_x + (v - V)U_x] = 0, \end{aligned} \tag{19}$$

$$
\begin{aligned}
&MU_{tt}-\frac{3}{4}(2C_1+3C_2)(u-U)+\frac{l}{4}(2C_1-9C_2)u_x-\frac{3l^2}{8}(2C_1+3C_2)u_{xx}+\frac{3M}{2}(U_{tt}-u_{tt})\\
&+\quad\frac{l^3}{24}(2C_1-9C_2)u_{xxx}-\frac{3Ml}{2}u_{xtt}-\frac{l^4}{32}(2C_1+3C_2)u_{xxxx}-\frac{3Ml^2}{4}u_{xxtt}\\
&\quad+\frac{81}{16l}C_2\big[(u-U)^2+2l(u-U)u_x\big]+\frac{3}{16l}(6C_1-7C_2)(v-V)^2-\frac{1}{8}(2C_1-21C_2)(v-V)v_x=0,
\end{aligned}\tag{20}
$$

$$
\begin{aligned}
&MV_{tt}-\frac{3}{4}(2C_1+C_2)(v-V)-\frac{3l}{4}(2C_1+C_2)v_x-\frac{3l^2}{8}(2C_1+C_2)v_{xx}-\frac{3M}{2}(v_{tt}-V_{tt})\\
&-\frac{l^3}{8}(2C_1+C_2)v_{xxx}+\frac{Ml}{2}v_{xtt}-\frac{l^4}{32}(2C_1+C_2)v_{xxxx}-\frac{3Ml^2}{4}v_{xxtt}+\frac{3\sqrt{3}}{2l}C_2[(v-V)^2-2l(v-V)v_x]\\
&+\frac{3}{8l}(6C_1-7C_2)(u-U)(v-V)+\frac{1}{8}(6C_1-21C_2)[(u-U)v_x+(v-V)u_x]=0.
\end{aligned}\tag{21}
$$

In the continuum limit sublattices are indistinguishable for an observer, and it no longer makes sense to use them for the description. An experimentalist can measure macrostrains in a continuum. The relative motion of the sublattices in the continuum is treated now as a microstructure. Therefore, new variables with such physical meaning are introduced.

The transformation of variables

$$
W=\frac{u+U}{2},\quad w=\frac{u-U}{2},\quad Q=\frac{v+V}{2},\quad q=\frac{v-V}{2},
$$

leads to the problem of describing the dynamics of the horizontal and vertical displacements W and Q and variables w, q, responsible for internal variations of a microstructure. Typical manipulations with Eqs. (18)–(21) result in equations with new variables:

$$
\begin{aligned}
&2MW_{tt}-\frac{3l^2}{4}(2C_1+3C_2)W_{xx}+\frac{l}{2}(2C_1-9C_2)w_x-3Mlw_{xtt}\\
&+\frac{l^3}{12}(2C_1-9C_2)w_{xxx}-\frac{3Ml^2}{2}W_{xxtt}-\frac{l^4}{16}(2C_1+3C_2)W_{xxxx}+\frac{81}{2}C_2\,ww_x+\frac{1}{2}(2C_1-21C_2)\,q\,q_x=0,
\end{aligned}\tag{22}
$$

$$
\begin{aligned}
&5Mw_{tt}+\frac{3l^2}{4}(2C_1+3C_2)w_{xx}+3(2C_1+3C_2)w-\frac{l}{2}(2C_1-9C_2)W_x\\
&+3MlW_{xtt}-\frac{l^3}{12}(2C_1-9C_2)W_{xxx}+\frac{3Ml^2}{2}w_{xxtt}+\frac{l^4}{16}(2C_1+3C_2)w_{xxxx}\\
&-\frac{2}{2l}(6C_1-7C_2)q^2-\frac{81}{2l}C_2\,w(w+l\,W_x)+\frac{1}{2}(2C_1-21C_2)\,q\,Q_x=0,
\end{aligned}\tag{23}
$$

$$
\begin{aligned}
&2MQ_{tt}-\frac{3l^2}{4}(2C_1+C_2)Q_{xx}+\frac{3l}{2}(2C_1+C_2)q_x+Mlq_{xtt}\\
&+\frac{l^3}{4}(2C_1+C_2)q_{xxx}-\frac{3Ml^2}{2}Q_{xxtt}-\frac{l^4}{16}(2C_1+C_2)Q_{xxxx}-4\sqrt{3}C_2\,qq_x+\frac{1}{2}(2C_1-21C_2)\,(w\,q)_x=0,
\end{aligned}\tag{24}
$$

$$
\begin{aligned}
&5Mq_{tt}-3(2C_1+C_2)q-\frac{3l^2}{4}(2C_1+C_2)q_{xx}+\frac{3l}{2}(2C_1+C_2)Q_x-MlQ_{xtt}\\
&+\frac{l^3}{4}(2C_1+C_2)Q_{xxx}+\frac{3Ml^2}{2}q_{xxtt}-\frac{l^4}{16}(2C_1+C_2)q_{xxxx}\\
&-\frac{12\sqrt{3}}{l}C_2q^2-\frac{3}{l}(7C_2-6C_1)q\,w-\frac{1}{2}(2C_1-21C_2)\,(wQ_x-qW_x)-4\sqrt{3}C_2q\,Q_x=0.
\end{aligned}\tag{25}
$$

For the weakly nonlinear case it is assumed that the strains are small, e.g., $W_x^2 \ll W_x$, and the long wavelength limit means that each derivative makes the term smaller, e.g., $W_{xxx} \ll W_{xx} \ll W_x$. The same estimations hold for w, Q, and q. One can check that the omitted terms in the discrete equations would result in the appearance of terms in the continuum equations that are smaller in comparison with the terms remaining there. When the order of smallness of higher order linear derivatives and order of smallness of nonlinear terms are dependent on each other, the nonlinearity can balance the dispersion. This phenomenon leads to a possible strain wave localization.

IV. INTERACTION OF LONGITUDINAL AND SHEAR WAVES

The standard perturbation methods involve obtaining an asymptotic solution for each variable order by order. An alternative way is to decrease the number of coupled equations by using the fact that the terms in Eqs. (22)–(25) can be of different order according to the aforementioned estimates. The procedure can be called the slaving principle. It was developed by Haken for the decoupling of nonlinear ordinary differential equations [28]. It was used earlier by the authors for the nonlinear coupled partial differential equations accounting for materials with a microstructure [29].

The separation by orders can be described by introducing the scales, e.g., the ratio of l and the scale for x. However, the combinations of the stiffnesses C_1 and C_2 in the expressions for the coefficients of the resulting equations could turn out small themselves, and this cannot be predicted in advance. That is why a dimensional analysis is preferable.

A. Slaving principle for obtaining governing equations

Assume that the solution w to Eq. (23) has the form

$$w = w_1 + w_2 + w_3 + \cdots, \tag{26}$$

where w_i are of different order. The order of w_1 relates to the highest order terms in Eq. (23),

$$3(2C_1 + 3C_2)w_1 - \frac{1}{2}(2C_1 - 9C_2)lW_x = 0,$$

which leads to the solution for w_1,

$$w_1 = \frac{l(2C_1 - 9C_2)W_x}{6(2C_1 + 3C_2)}. \tag{27}$$

Similarly, the solution q to Eq. (25) has the form

$$q = q_1 + q_2 + q_3 + \cdots, \tag{28}$$

and the leading-order solution q_1 is

$$q_1 = \frac{l}{2} Q_x. \tag{29}$$

The next-order solution w_2 to Eq (23) is expressed through the next-order terms taking into account Eqs. (27) and (29),

$$w_2 = \alpha_1 W_x^2 + \alpha_2 Q_x^2 + \alpha_3 W_{xtt} + \alpha_4 W_{xxxx}, \tag{30}$$

where

$$\alpha_1 = \frac{3C_2 l(2C_1 - 9C_2)(14C_1 + 9C_2)}{8(2C_1 + 3C_2)^3}, \quad \alpha_2 = \frac{7l}{24},$$
$$\alpha_3 = -\frac{Ml(46C_1 + 9C_2)}{18(2C_1 + 3C_2)^2}, \quad \alpha_4 = -\frac{l^3(2C_1 - 9C_2)}{72(2C_1 + 3C_2)}.$$

Similarly, the next-order solution q_2 to Eq. (25) is

$$q_2 = \beta_1 W_x Q_x + \beta_2 Q_x^2 + \beta_3 Q_{xxx} + \beta_4 Q_{xtt}, \tag{31}$$

where

$$\beta_1 = \frac{l(44C_1^2 - 252C_1C_2 - 189C_2^2)}{36(2C_1 + C_2)(2C_1 + 3C_2)}, \quad \beta_2 =, -\frac{5C_2 l}{\sqrt{3}(2C_1 + C_2)},$$
$$\beta_3 = -\frac{l^3}{24}, \quad \beta_4 = \frac{M}{2(2C_1 + C_2)}.$$

By substituting Eqs.(27), (30), (29), and (31) into Eqs. (22) and (24) one obtains coupled equations for longitudinal and shear waves,

$$2MW_{tt} - \gamma_1 W_{xx} - \gamma_2 (W_x^2)_x - \gamma_3 (Q_x^2)_x - \gamma_4 W_{xxxx} - \gamma_5 W_{xxtt} = 0, \tag{32}$$

$$2MQ_{tt} - \delta_2 (W_x Q_x)_x - \delta_3 (Q_x^2)_x - \delta_4 Q_{xxxx} - \delta_5 Q_{xxtt} = 0, \tag{33}$$

where $\gamma_i = \gamma_i(C_1, C_2)$, $\delta_i = \delta_i(C_1, C_2)$,

$$\gamma_1 = \frac{4l^2 C_1(2C_1 + 9C_2)}{3(2C_1 + 3C_2)},$$
$$\gamma_2 = \frac{3l^2 C_2(2C_1 - 9C_2)^2(10C_1 + 9C_2)}{8(2C_1 + 3C_2)^3},$$
$$\gamma_3 = \frac{l^2}{24}(10C_1 - 63C_2),$$
$$\gamma_4 = \frac{l^4}{144(2C_1 + 3C_2)}(20C_1^2 + 60C_1C_2 + 153C_2^2),$$
$$\gamma_5 = \frac{Ml^2}{4(2C_1 + 3C_2)^2}(28C_1^2 + 68C_1C_2 - 9C_2^2),$$
$$\delta_2 = \frac{l^2 C_1}{2C_1 + 3C_2}(13C_2 - 2C_1), \quad \delta_3 = -3\sqrt{3}l^2 C_2,$$
$$\delta_4 = -\frac{l^4}{8}(2C_1 + C_2), \quad \delta_5 = \frac{11Ml^2}{4}.$$

The stiffnesses C_1, C_2 are positive. Then one can see that $\gamma_1 > 0$, $\gamma_2 > 0$, $\gamma_4 > 0$, while γ_3 and γ_5 can be of either sign as well as δ_2. The remaining coefficients $\delta_3 < 0$, $\delta_4 < 0$, $\delta_5 > 0$.

B. Exact localized longitudinal strain wave solution

In the absence of shear displacements, $Q = 0$, Eqs. (32) and (33) are reduced to a single equation for the longitudinal strains $F = W_x$,

$$2MF_{tt} - \gamma_1 F_{xx} - \gamma_2 (F^2)_{xx} - \gamma_4 F_{xxxx} - \gamma_5 F_{xxtt} = 0. \tag{34}$$

Note that the nonlinearity arises for nonzero γ_2 or in the presence of the angular stiffness C_2. Its traveling wave solution depending on the phase variable $x - Vt$ can be obtained by direct integration. In particular, the localized strain wave solution is

$$F = A\,\text{sech}^2[k(x - Vt - x_0)], \tag{35}$$

where

$$A = \frac{3(2MV^2 - \gamma_1)}{2\gamma_2}, \quad k^2 = \frac{2MV^2 - \gamma_1}{4(\gamma_4 + \gamma_5 V^2)}, \tag{36}$$

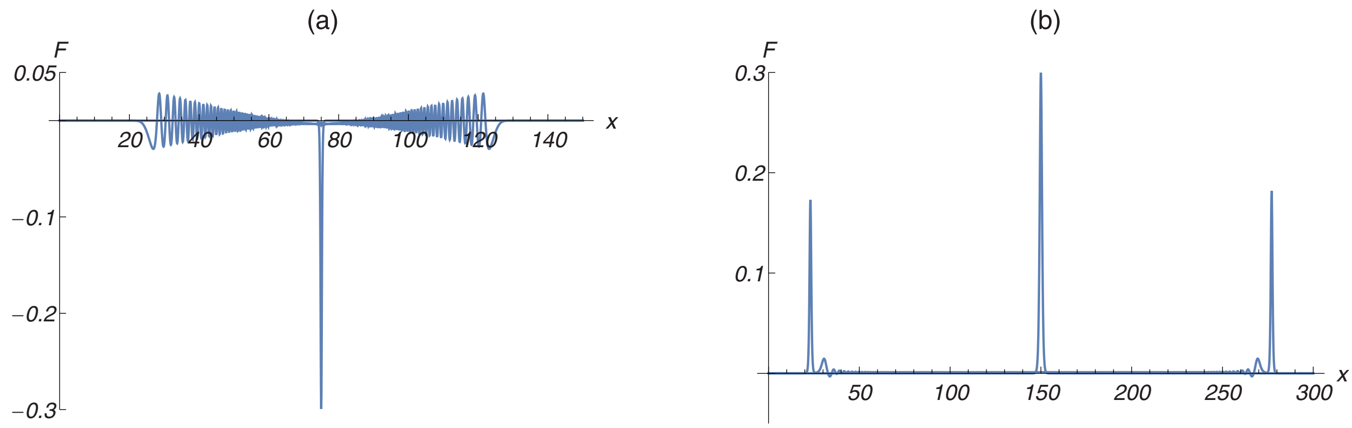

FIG. 4. Evolution of a longitudinal strain wave at different sign of the amplitude of the initial condition. (a) Delocalization of a negative amplitude input due to dispersion. (b) Splitting of a positive amplitude input into two localized waves of permanent shape and velocity due to a balance between nonlinearity and dispersion.

where $x_0 = \text{const}$ is the initial phase and V is a free parameter.

The wave number, k, should be real, and the expression under the square root should be positive. Hence, according to the definition of $\gamma' s$, $\gamma_5 > 0$ for $C_1 > (4\sqrt{22} - 17)C_2/14$. Then a real value of k is achieved at the velocity $V > \sqrt{\gamma_1/(2M)}$, and the amplitude, A, is always positive corresponding to a tensile strain wave. For $0 < C_1 < (4\sqrt{22} - 17)C_2/14$, $\gamma_5 < 0$. One can check that $\gamma/(2M) < -\gamma_4/\gamma_5$, and k is real if the velocities are from the interval $\sqrt{\gamma_1/(2M)} < V < \sqrt{-\gamma_4/\gamma_5}$. Again the amplitude A is always positive in this case, and no localized longitudinal compression strain wave exists due to the geometrical nonlinearity.

The solution (35) requires specific initial conditions for its existence in the form of the solution at $t = 0$ and its first temporal derivative at $t = 0$. However, the aforementioned analysis about the possible sign of the amplitude of longitudinal strain wave remains valid in a more general case solved numerically. Shown in Fig. 4 are two numerical solutions to Eq. (34) describing the evolution of an initially motionless localized pulse having negative or positive amplitude. One can see in Fig. 4(a) two profiles, the initial pulse and the waves at some later time. The negative amplitude pulse splits into two oscillating waves propagating in the opposite directions. Dispersion destroys the localization of the initial pulse. On the other hand, the positive amplitude pulse shown in Fig. 4(b) splits into two localized waves of the shape that is kept in time. One can check that each of these waves is described by the exact solution (35).

C. Exact localized strain wave solution to the coupled equation for longitudinal and shear waves

Equations (32) and (33) can be rewritten for longitudinal and shear strains, $P = W_x$, $S = Q_x$:

$$2MP_{tt} - \gamma_1 P_{xx} - \gamma_2 (P^2)_x - \gamma_3 (S^2)_x - \gamma_4 P_{xxxx} - \gamma_5 P_{xxtt} = 0, \tag{37}$$

$$2MS_{tt} - -\delta_2 (PS)_x - \delta_3 (S^2)_x - \delta_4 S_{xxxx} - \delta_5 S_{xxtt} = 0. \tag{38}$$

The ansatz for localized strain wave solution is

$$P = A\,\text{sech}^2[k(x - Vt - x_0)],$$
$$S = AB\,\text{sech}^2[k(x - Vt - x_0)] + S_0, \tag{39}$$

where x_0 is the initial phase and S_0 is a constant accounting for a shear pre-stress. This constant provides a free parameter in the solution (39), like the velocity V in the solution for longitudinal waves (35) and (36). The amplitude in the form of the product $A \times B$ for the wave S is chosen instead of B in order to obtain more compact relationships for the parameters of the ansatz (39).

We substitute Eq. (39) into Eqs. (37), (38). The derivatives of the hyperbolic secant function can be expressed through powers of itself. To solve the obtained equation, the terms at the same powers of hyperbolic secant function are assumed to be zero. This leads to the system of coupled algebraic equations for the constants of solution (39). Thus the system obtained for the factor $\text{sech}^2[k(x - Vt - x_0)]^4$ is

$$A\gamma_2 + AB^2\gamma_3 - 6k^2(\gamma_4 + \gamma_5 V^2) = 0, \tag{40}$$

$$A\delta_2 + AB\delta_3 - 6k^2(\delta_4 + \delta_5 V^2) = 0. \tag{41}$$

For the factor $\text{sech}^2[k(x - Vt - x_0)]^2$ the system reads

$$\gamma_1 + 4\gamma_4 k^2 - 2(M - 2\gamma_5 k^2)V^2 = 0, \tag{42}$$

$$S_0\delta_2 + B[\delta_1 + 4\delta_4 k^2 - 2(M - 2\delta_5 k^2)V^2] = 0. \tag{43}$$

The last equation leads to the solution for the shear prestress, S_0,

$$S_0 = -\frac{B}{\delta_2}[\delta_1 + 4\delta_4 k^2 - 2(M - 2\delta_5 k^2)V^2].$$

The wave number k is defined from Eq. (42),

$$k^2 = \frac{2MV^2 - \gamma_1}{4(\gamma_4 + \gamma_5 V^2)},$$

which is the same as for the solution Eq. (35) for longitudinal waves. Therefore the analysis of the reality of k (36) remains valid. The amplitude of longitudinal wave, A, is obtained from

Eq. (40),

$$A = \frac{3(2MV^2 - \gamma_1)}{2(\gamma_2 + B^2\gamma_3)}.$$

Comparing it with Eq. (36) one can find a possible change of the sign of the amplitude A at $\gamma_3 < 0$. One can note that the negative γ_3 is achieved only in the presence of angular stiffness C_2 when $C_1 < 63C_2/10$. Then A may be negative for $V > \sqrt{\gamma_1/(2M)}$ and $B > -\gamma_2/\gamma_3$. The parameter B is found from the quadratic algebraic equation, which follows from Eq. (41),

$$B^2\gamma_3(\delta_4 + \delta_5V^2) - B\delta_3(\gamma_4 + \gamma_5V^2) + \gamma_2(\delta_4 + \delta_5V^2) - \delta_2(\gamma_4 + \gamma_5V^2) = 0.$$

Then each localized longitudinal strain wave with the amplitude A can be accompanied by two shear waves with the amplitude $A \times B$.

Due to the rich dynamics revealed on the basis of the traveling wave solution a more complicated numerical study is needed for the coupled equations. However, it is not suitable to add it to this paper.

V. CONCLUSIONS

A geometrically nonlinear model of a hexagonal 2D lattice was developed in order to obtain coupled nonlinear equations for longitudinal and shear strain dynamics. The asymptotic procedure developed allowed us to keep the most important nonlinear and dispersion terms in the equations. It provided a balance between nonlinearity and dispersion giving rise to localized strain existence. The localized strain waves may propagate keeping their shape and velocity. This is important for problems of nondestructive testing and durability of materials. It also might be useful for a development of the new heat conduction models based on the analysis of the nonlinear crystalline lattice.

Of special interest is the role of angular stiffness in the lattice model. It entirely provides a nonzero quadratic nonlinear term in continuum limit Eq. (34) for pure longitudinal waves as happens in pure continuum modeling. In the absence of shear waves, only a tensile localized longitudinal strain wave (35) may propagate. A compression wave may appear if the physical nonlinearity is taken into account [30]. The solution (39) for the waves' interaction keeps the interval for permitted velocities but, however, adds the possibility of a compression longitudinal strain wave, even in the absence of the physical nonlinearity. Also the solution predicts the coexistence of interacting longitudinal and shear waves when two shear waves may correspond to the longitudinal one.

One should note the important role of the constant prestress S_0 in the existence of the interacting localized waves. In its absence the velocity is fixed as follows from Eq. (43). The prestress affects the shear strain and could act as a control of it giving rise, in turn, variation in the sign of the amplitude of longitudinal wave A.

It would be interesting to provide estimations based on the values of the parameters of the model. However, there is a lack in numerical data for the parameters, especially, about l and C_2. Possible future work concerns numerical simulations of coupled equations and consideration of 2D instability of plane strain waves.

ACKNOWLEDGMENTS

This work was performed at IPME RAS and at TU Berlin, supported by a joint grant from the Russian Science Foundation (Grant No. 19-41-04106) and the German Research Foundation (DFG) (Grants No. MU 1752/50-1 and No. 405631704).

APPENDIX: PARTS OF EQS. (13)–(16)

The Appendix contains detailed expressions for the linear discrete parts, $L_j(x, X, y, Y)$, the linear differential-discrete parts, $D_j(x, X, y, Y)$, and the nonlinear discrete parts, $N_j(x, X, y, Y)$, $j = 1–4$, in the equations of motion (13)–(16).

$$\begin{aligned}
L_1(x, X, y, Y) = {}& \frac{C_1}{4}[4(X_{m+1,n} - x_{m,n}) + X_{m-1,n+1} - 2x_{m.n} + X_{m-1,n-1} \\
& + \sqrt{3}(Y_{m-1,n-1} - Y_{m-1,n+1})] + \frac{3\sqrt{3}C_2}{8}[(Y_{m-1,n-1} - Y_{m-1,n+1}) + \sqrt{3}(X_{m-1,n+1} - 2x_{m.n} + X_{m-1,n-1})],\\
D_1(x, X, y, Y) = {}& \frac{\sqrt{3}M}{4}[\sqrt{3}(\ddot{X}_{m-1,n+1} - 2\ddot{x}_{m.n} + \ddot{X}_{m-1,n-1}) + \ddot{Y}_{m-1,n+1} - \ddot{Y}_{m-1,n-1}],\\
N_1(x, X, y, Y) = {}& \frac{C_1}{16l}\{8(Y_{m+1,n} - y_{m,n})^2 + 5[(Y_{m+1,n-1} - y_{m,n})^2 + (Y_{m+1,n+1} - y_{m,n})^2]\\
& + 2\sqrt{3}[(X_{m+1,n+1} - x_{m.n})(Y_{m-1,n+1} - y_{m.n}) - (X_{m-1,n-1} - x_{m.n})(Y_{m-1,n-1} - y_{m.n})]\}\\
& + \frac{C_2}{32l}\{81[(X_{m-1,n-1} - x_{m,n})^2 + (X_{m-1,n+1} - x_{m,n})^2] - 21[(Y_{m-1,n-1} - y_{m,n})^2 + (Y_{m-1,n+1} - y_{m,n})^2]\\
& \times 6\sqrt{3}[(X_{m-1,n+1} - x_{m,n})(Y_{m-1,n+1} - y_{m,n}) - (X_{m-1,n-1} - x_{m,n})(Y_{m-1,n-1} - y_{m,n})]\},
\end{aligned}$$

$$L_2(x,X,y,Y) = \frac{\sqrt{3}C_1}{4}[X_{m-1,n-1} - X_{m-1,n+1} + \sqrt{3}(Y_{m-1,n-1} - 2y_{m,n} + Y_{m-1,n+1})] + \frac{3C_2}{8}[\sqrt{3}(X_{m-1,n+1} - X_{m-1,n-1}) + (Y_{m-1,n-1} - 2y_{m,n} + Y_{m-1,n+1})],$$

$$D_2(x,X,y,Y) = \frac{M}{4}[(\ddot{Y}_{m-1,n+1} - 2\ddot{y}_{m.n} + \ddot{Y}_{m-1,n-1}) + 4(\ddot{Y}_{m+1.n} - \ddot{y}_{m.n}) + \sqrt{3}(\ddot{X}_{m-1,n-1} - \ddot{X}_{m-1,n+1})],$$

$$\begin{aligned} N_2(x,X,y,Y) = {} & \frac{C_1}{12l}\{\sqrt{3}[(X_{m-1,n+1} - x_{m,n})^2 - (X_{m-1,n-1} - x_{m,n})^2] \\ & + 10[(X_{m-1,n-1} - x_{m,n})(Y_{m-1,n-1} - y_{m,n}) + (X_{m-1,n+1} - x_{m,n})(Y_{m-1,n+1} - y_{m,n})] \\ & + 16(X_{m+1,n} - x_{m,n})(Y_{m+1,n} - y_{m,n})\} \\ & + \frac{\sqrt{3}C_2}{32}\{3[(X_{m-1,n+1} - x_{m,n})^2 - (X_{m-1,n-1} - x_{m,n})^2] + 15[(Y_{m-1,n-1} - y_{m,n})^2 - (Y_{m-1,n+1} - y_{m,n})^2] \\ & + 16(Y_{m+1,n} - y_{m,n})^2 - 14\sqrt{3}[(X_{m-1,n-1} - x_{m,n})(Y_{m-1,n-1} - y_{m,n}) \\ & + (X_{m-1,n+1} - x_{m,n})(Y_{m-1,n+1} - y_{m,n})] + 16\sqrt{3}[(X_{m-1,n+1} - x_{m,n})(Y_{m+1,n} - y_{m,n}) \\ & - (X_{m-1,n-1} - x_{m,n})(Y_{m+1,n} - y_{m,n})] + 16(Y_{m+1,n} - y_{m,n})(Y_{m-1,n-1} - 2y_{m,n} + Y_{m-1,n+1})\}, \end{aligned}$$

$$\begin{aligned} L_3(x,X,y,Y) = {} & \frac{C_1}{4}[4(x_{m-1,n} - X_{m,n}) + x_{m+1,n+1} - 2X_{m.n} + x_{m+1,n-1} \\ & + \sqrt{3}(y_{m+1,n+1} - y_{m+1,n-1})] + \frac{3\sqrt{3}C_2}{8}[(y_{m+1,n-1} - y_{m+1,n+1}) + \sqrt{3}(x_{m+1,n+1} - 2X_{m.n} + x_{m+1,n-1})], \end{aligned}$$

$$D_3(x,X,y,Y) = \frac{\sqrt{3}M}{4}[\sqrt{3}(\ddot{x}_{m+1,n+1} - 2\ddot{X}_{m.n} + \ddot{x}_{m+1,n-1}) + \ddot{y}_{m-1,n+1} - \ddot{y}_{m+1,n+1}],$$

$$\begin{aligned} N_3(x,X,y,Y) = {} & -\frac{C_1}{16l}\{8(y_{m-1,n} - Y_{m,n})^2 + 5[(y_{m+1,n-1} - Y_{m,n})^2 + (y_{m+1,n+1} - Y_{m,n})^2] \\ & + 2\sqrt{3}[(x_{m+1,n-1} - X_{m.n})(y_{m+1,n+1} - Y_{m.n}) - (x_{m-1,n+1} - X_{m.n})(y_{m+1,n-1} - Y_{m.n})]\} \\ & + \frac{C_2}{32l}\{-81[(x_{m+1,n-1} - X_{m,n})^2 + (x_{m+1,n+1} - X_{m,n})^2] + 21[(y_{m+1,n-1} - Y_{m,n})^2 + (y_{m+1,n+1} - Y_{m,n})^2] \\ & \times 6\sqrt{3}[(x_{m+1,n+1} - X_{m,n})(y_{m+1,n+1} - Y_{m,n}) - (x_{m+1,n-1} - X_{m,n})(y_{m+1,n-1} - Y_{m,n})]\}, \end{aligned}$$

$$L_4(x,X,y,Y) = \frac{\sqrt{3}C_1}{4}[x_{m+1,n+1} - x_{m+1,n-1} + \sqrt{3}(y_{m+1,n-1} - 2Y_{m,n} + y_{m+1,n+1})] + \frac{3C_2}{8}[\sqrt{3}(x_{m+1,n-1} - x_{m+1,n+1}) + y_{m+1,n-1} - 2Y_{m,n} + y_{m+1,n+1}],$$

$$D_4(x,X,y,Y) = \frac{M}{4}[(\ddot{y}_{m+1,n+1} - 2\ddot{Y}_{m.n}) + \ddot{y}_{m+1,n-1} + 4(\ddot{y}_{m-1.n} - \ddot{Y}_{m.n}) + \sqrt{3}(\ddot{x}_{m+1,n-1} - \ddot{x}_{m+1,n+1})]$$

$$\begin{aligned} N_4(x,X,y,Y) = {} & \frac{C_1}{16l}\{\sqrt{3}[(x_{m+1,n+1} - X_{m,n})^2 - (x_{m+1,n-1} - X_{m,n})^2] - 10[(x_{m+1,n-1} - X_{m,n})(y_{m+1,n-1} - Y_{m,n}) \\ & + (x_{m+1,n+1} - X_{m,n})(y_{m+1,n+1} - Y_{m,n})] - 16(x_{m-1,n} - X_{m,n})(y_{m-1,n} - Y_{m,n})\} \\ & + \frac{\sqrt{3}C_2}{32}\{3[(x_{m+1,n+1} - X_{m,n})^2 - (x_{m+1,n-1} - X_{m,n})^2] + 15[(y_{m+1,n-1} - Y_{m,n})^2 - (y_{m+1,n+1} - Y_{m,n})^2] \\ & - 16(y_{m-1,n} - Y_{m,n})^2 + 14\sqrt{3}[(x_{m+1,n-1} - X_{m,n})(y_{m+1,n-1} - Y_{m,n}) \\ & + (x_{m+1,n+1} - X_{m,n})(y_{m-1,n+1} - Y_{m,n})] + 16\sqrt{3}[(x_{m+1,n+1} - X_{m,n})(y_{m-1,n} - Y_{m,n}) \\ & - (x_{m+1,n-1} - X_{m,n})(y_{m-1,n} - y_{m,n})] - 16(y_{m-1,n} - Y_{m,n})(y_{m+1,n-1} - 2Y_{m,n} + y_{m+1,n+1})\}. \end{aligned}$$

[1] M. Born and K. Huang, *Dynamic Theory of Crystal Lattices* (Clarendon Press, Oxford, 1954).

[2] A. I. Manevich and L. I. Manevitch, *The Mechanics of Nonlinear Systems with Internal Resonances* (Imperial College Press, London, 2005).

[3] M. Ostoja-Starzewski, Lattice models in micromechanics, Appl. Mech. Rev. **55**, 35 (2002).

[4] A. Askar, *Lattice Dynamical Foundations of Continuum Theories* (World Scientific, Singapore, 1985).

[5] G. A. Maugin, *Nonlinear Waves in Elastic Crystals* (Oxford University Press, Oxford, 1999).

[6] I. V. Andrianov, J. Awrejcewicz, and D. Weichert, Improved continuous models for discrete media, Math. Prob. Eng. **2010**, 986242 (2009).

[7] S. Lepri, editor, *Thermal Transport in Low Dimensions: From Statistical Physics to Nanoscale Heat Transfer*, Lecture Notes in Physics Vol. 921 (Springer International Publishing, Cham, 2016).

[8] A. M. Krivtsov, The ballistic heat equation for a one-dimensional harmonic crystal, in *Dynamical Processes in Generalized Continua and Structures*, edited by H. Altenbach, A. Belyaev, V. A. Eremeyev, A. Krivtsov, and A. V. Porubov, Advanced Structured Materials Vol. 103 (Springer Nature, Cham, 2019), p. 345.

[9] A. A. Sokolov, A. M. Krivtsov, W. H. Müller, and E. N. Vilchevskaya, Change of entropy for the one-dimensional ballistic heat equation: Sinusoidal initial perturbation, Phys. Rev. E **99**, 042107 (2019).

[10] E. Barani, I. P. Lobzenko, E. A. Korznikova, E. G. Soboleva, S. V. Dmitriev, K. Zhou, and A. M. Marjaneh, Transverse discrete breathers in unstrained graphene, Eur. Phys. J. B **90**, 38 (2017).

[11] A. I. Lurie, *Nonlinear Theory of Elasticity* (Elsevier, Amsterdam, 1990).

[12] H. M. Shodja and M. R. Delfani, A novel nonlinear constitutive relation for graphene and its consequence for developing closed-form expressions for Young's modulus and critical buckling strain of single-walled carbon nanotubes, Acta Mech. **222**, 91 (2011).

[13] X. Wei, B. Fragneaud, C. A. Marianetti, and J. W. Kysar, Nonlinear elastic behavior of graphene: *Ab initio* calculations to continuum description, Phys. Rev. B **80**, 205407 (2009).

[14] T. Yu. Astakhova, O. D. Gurin, M. Menon, and G. A. Vinogradov, Longitudinal solitons in carbon nanotubes, Phys. Rev. B, **64**, 035418 (2001).

[15] P. Zhang, Y. Huang, P. H. Guebelle, P. A. Klein, and K. Hwang, The elastic modulus of single-wall carbon nanotubes: A continuum analysis incorporating interactomic potentials, Intl. J. Solids Struct. **39**, 3893 (2002).

[16] Y. Huang, J. Wu, and K. C. Hwang, Thickness of graphene and single-wall carbon nanotubes, Phys. Rev. B **74**, 245413 (2006).

[17] A. Porubov and I. Berinskii, Non-linear plane waves in materials having hexagonal internal structure, Intl. J. Non-Linear Mech. **67**, 27 (2014).

[18] A. V. Porubov, A. M. Krivtsov, and A. E. Osokina, Two-dimensional waves in extended square lattice, Intl. J. Non-Linear Mech. **99**, 281 (2018).

[19] K. Khusnutdinova, A. M. Samsonov, and A. S. Zakharov, Nonlinear layered lattice model and generalized solitary waves in imperfectly bonded structures, Phys. Rev. E **79**, 056606 (2009).

[20] M. K. Sayadi and J. Pouget, Soliton dynamics in a microstructured lattice model, J. Phys. A: Math. Gen. **24**, 2151 (1991).

[21] S. P. Wallen and M. R. Haberman, Nonreciprocal wave phenomena in spring-mass chains with effective stiffness modulations induced by geometrical nonlinearity, Phys. Rev. E **99**, 013001 (2019).

[22] H. Askes and A. Metrikine. Higher-order continua derived from discrete media: Continualisation aspects and boundary conditions, Intl. J. Solids Struct. **42**, 187 (2005).

[23] A. V. Metrikine and H. Askes. An isotropic dynamically consistent gradient elasticity model derived from a 2D lattice, Phil. Mag. **86**, 3259 (2006).

[24] A. A. Vasiliev, S. V. Dmitriev, and A. E. Miroshnichenko, Mutlti-field continuum theory for medium with microscopic rotations, Intl. J. Solids Struct. **42**, 6245 (2005).

[25] A. Genoese, A. Genoese, N. L. Rizzi, and G. Salerno, On the derivation of the elastic properties of lattice nanostructures: The case of graphene sheets, Composites Part B: Eng. **115**, 316 (2017).

[26] J. L. Ericksen, On the Cauchy–Born Rule, Math. Mech. Solids **13**, 199 (2008).

[27] Zh. Peng, H. Youggang, P. H. Geubelle, and H. Kelichikh, On the continuum modelling of carbon nanotubes, Acta Mech. Sinica **18**, 528 (2002).

[28] H. Haken, *Advanced Synergetics* (Springer-Verlag, Berlin, 1983).

[29] A. V. Porubov and F. Pastrone, Nonlinear bell-shaped and kink-shaped strain waves in microstructured solids Intern, J. Non-Linear Mech. **39**, 1289 (2004).

[30] A. V. Porubov and A. E. Osokina, Double dispersion equation for nonlinear waves in a graphene-type hexagonal lattice, Wave Motion **89**, 185 (2019).